INT. J. ELECTRONICS, 1998, VOL. 85, NO. 3, 293–312

Generation of CCII and CFOA filters from passive *RLC* filters

AHMED M. SOLIMAN†

It is shown that low-sensitivity active filters employing the current conveyor (CCII) or the current feedback operational amplifier (CFOA) as the active element can be generated directly from passive *RLC* filters. New current-mode filters using CCII and voltage mode filters using the CFOA are generated from three alternative passive *RLC* filters. The proposed circuits have the advantage that compensation of the dominant parasitic elements of the CCII or the CFOA can be easily achieved. PSpice simulation results are included.

1. Introduction

Several active filters have been introduced in the literature using the second-generation current conveyor (CCII) (Sedra and Smith 1970) or the current feedback operational amplifier (CFOA) as active elements. Some of these filters are generated from op amp filters using some form of transformation (Roberts and Sedra 1992, Svoboda 1989, Soliman 1994, 1995, 1996 a). A very large number of CCII filters have been introduced in the literature (Chang and Chen 1991, Chang *et al.* 1994, Sun and Fidler 1994, Higashimura and Fukui 1996). Most of these CCII filters are given in a direct form without identifying the generation method or an equivalent op amp filter or a passive *RLC* filter, if it exists. Several authors have also proposed active *RC* filters using the CFOA as the active element (Fabre 1992, 1993, Liu 1995 a, b, Soliman 1996 b, Abuelmatti and Al-Shahrani 1996), while other authors have reported active-*R* filters using the CFOA (Payne and Toumazou 1995).

The low-sensitivity passive *RLC* filters will remain as a basic starting point to generate low-sensitivity active filters. The purpose of this paper is to support this statement and to bridge the gap between passive filters and CCII and CFOA filters, bypassing the op amp filters. Several current-mode CCII filters as well as voltage-mode CFOA filters are generated directly from three alternative forms of passive *RLC* filter.

The first part of the paper includes minimum passive component ($2R+2C$) current-mode filters using CCII and voltage-mode filters using the CFOA, that are generated from two alternative configurations of the second-order passive *RLC* filter. A third form of passive *RLC* filter is shown to be capable of generating current-mode $3R+2C$ bandpass filters having independent control on Q and using CCII, as well as a voltage-mode bandpass-lowpass filter using the CFOA. Compensation of the parasitic parameters of the CCII and the CFOA are considered. PSpice simulation results are included, showing the excellent performance of the proposed compensated filters. It should be noted that some of the filters described in this paper have been reported before based on alternative methods of circuit generation.

Received 20 May 1997; accepted 27 August 1997.

† Electronics and Communication Engineering Department, Cairo University, Giza, Egypt.

2. The $2R + 2C$ filters

In this section the minimum *RC* bandpass-lowpass filters using the CCII or the CFOA are considered. Filters realizing voltage transfer functions (voltage-mode filters) as well as current-mode filters, realizing current transfer functions are generated from the passive *RLC* filters of figures 1(*a*) and (*b*), respectively.

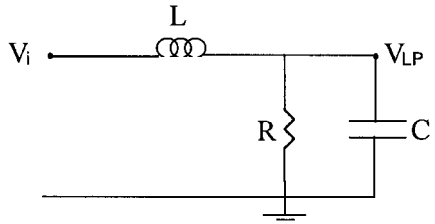

(*a*)

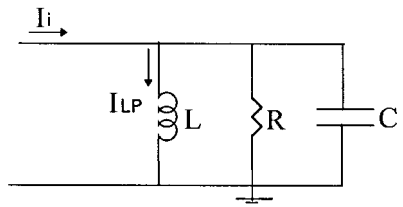

(*b*)

Figure 1. (*a*) Voltage-mode passive *RLC* lowpass filter; (*b*) current-mode passive *RLC* lowpass filter.

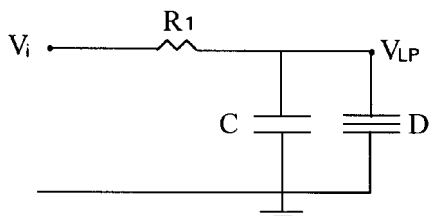

(*a*)

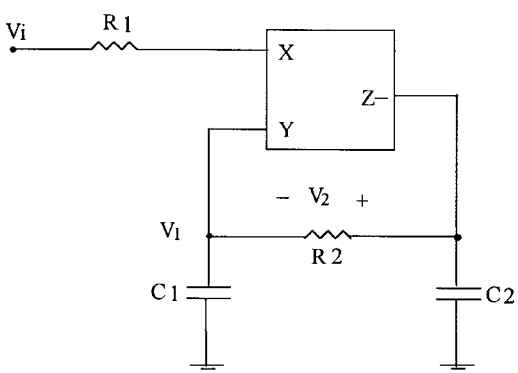

(*b*)

Figure 2. (*a*) Voltage-mode active *RCD* lowpass filter; (*b*) voltage-mode grounded-*C* lowpass filter using CCII- .

2.1. *Voltage-mode filters*

Consider first the passive *RLC* lowpass filter shown in figure 1(*a*). Apply the Bruton (1969) transformation; the active *RCD* lowpass filter shown in figure 2(*a*) is obtained. The well-known grounded-capacitor parallel CD circuit using a CCII- (Soliman 1978) is used here, resulting in the lowpass filter in figure 2(*b*), whose transfer function is given by

$$\frac{V_1}{V_i} = \frac{1}{s^2 C_1 C_2 R_1 R_2 + s(C_1 + C_2) R_1 + 1} \tag{1}$$

This ground-capacitor unity DC gain lowpass filter is very attractive for low Q applications. For a specified ω_0 and Q, the design equations are given by

$$C_1 = C_2 = C \tag{2}$$

$$R_1 = \frac{1}{2Q\omega_0 C} \quad \text{and} \quad R_2 = \frac{2Q}{\omega_0 C} \tag{3}$$

A close look at the circuit of figure 2(*b*) indicates that the floating voltage V_2 has a bandpass nature. In order to generate a practical bandpass filter based on this property a second CCII- acting as a current follower is added to the circuit, resulting in a virtual ground at the left terminal of R_2; thus a bandpass response is obtained at the other terminal of R_2, as shown in figure 3(*a*). The bandpass and the lowpass transfer functions of this circuit are given, respectively, by

$$\frac{V_{BP}}{V_i} = \frac{sC_1 R_2}{s^2 C_1 C_2 R_1 R_2 + sC_1 R_1 + 1} \tag{4}$$

$$\frac{V_{LP}}{V_i} = \frac{1}{s^2 C_1 C_2 R_1 R_2 + sC_1 R_1 + 1} \tag{5}$$

It is seen that the ω_0 and the Q sensitivities to all passive circuit components are equal to ± 0.5. For a specified ω_0 and Q, the design equations based on equal-R or equal-C can easily be obtained. However, in order to limit the resistor ratio and the capacitor ratio to Q, the design equations are taken as

$$C_2 = QC_1 \tag{6}$$

$$R_1 = \frac{1}{Q\omega_0 C_1} \quad \text{and} \quad R_2 = \frac{1}{\omega_0 C_1} \tag{7}$$

where the magnitude of C_1 is chosen to be much larger than the stray capacitance at port Z of the CCII (C_Z), in order to minimize the effect of C_Z on the filter performance.

The bandpass center frequency gain is equal to Q, and the lowpass DC gain is equal to unity. The circuit of figure 3(*a*) can be converted to realize an inverting bandpass filter by replacing both the CCII- by two CCII+, resulting in the circuit shown in figure 3(*b*). The design equations for this circuit are the same as given by (6) and (7).

A novel inverting-bandpass, non-inverting-lowpass filter based on the circuit of figure 3(*b*), and using two CFOA is shown in figure 4. This circuit has the same design equations given by (6) and (7) and has the advantage over the circuit of figure 3(*b*) in having buffered outputs. This $2R + 2C$ bandpass-lowpass filter has the

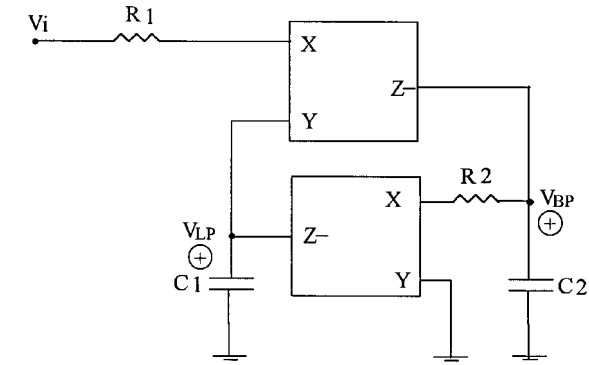

(*a*)

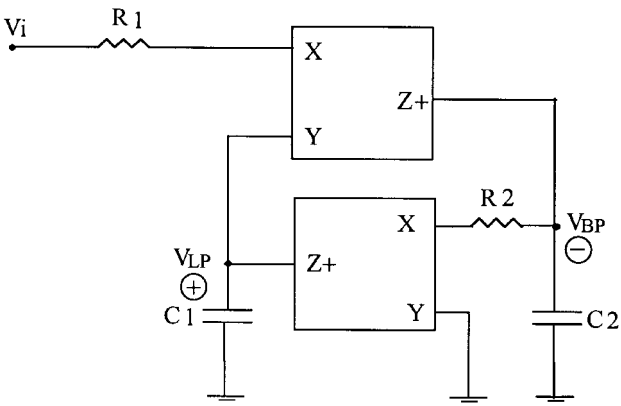

(*b*)

Figure 3. (*a*) Voltage-mode bandpass-lowpass filter using two CCII-; (*b*) voltage-mode bandpass-lowpass filter using two CCII+.

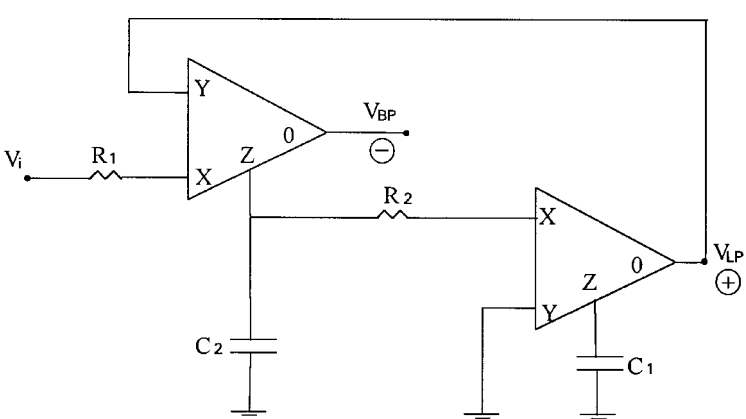

Figure 4. New inverting bandpass, non-inverting lowpass filter using CFOAs.

attractive advantage that the effect of C_Z and R_X of both the CFOAs can be absorbed in the four passive circuit components. It should be noted that this filter circuit is new and is not among the family of the bandpass-lowpass filters reported recently (Soliman 1996 b).

It has been demonstrated that the $2R+2C$ voltage-mode bandpass-lowpass filter using the CFOAs is more practical than the corresponding CCII filters due to the buffered outputs. To realize current transfer functions however, the CCII remains the most versatile active building block, as explained next.

2.2. *Current-mode filters*

Apply the Bruton (1969) transformation to the passive *RLC* filter of figure 1(*b*); the circuit of figure 5(*a*) is obtained. Using the CCII realization of the parallel CD circuit (Soliman 1978) results in the circuit of figure 5(*b*). The current I_1 has a low-pass nature and can easily be used, by adding a second CCII acting as a current follower at the grounded terminal of R_1. The current, I_2, however, has a bandpass nature, but it cannot be used in the circuit's present form. In order to achieve a practical bandpass output current, a second CCII is added to the circuit, acting as a voltage follower between ports Y and X, as shown in figure 6(*a*).The output current of this circuit, which is the same as the current in R_2, remains as a bandpass response. It should be noted that the addition of this second CCII to the circuit not only provides the physical output current from its Z port, but also results in a

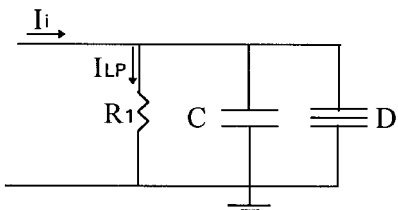

(*a*)

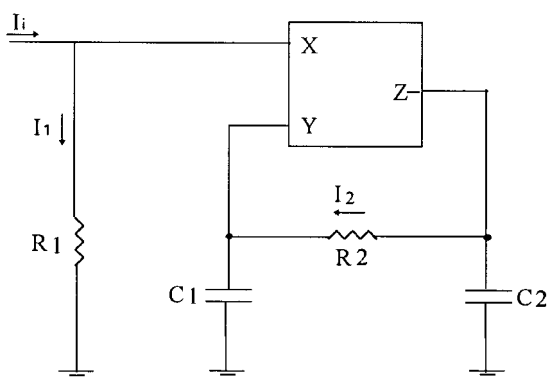

(*b*)

Figure 5. (*a*) Current-mode active *RCD* lowpass filter; (*b*) current-mode grounded-*C* lowpass filter using CCII- .

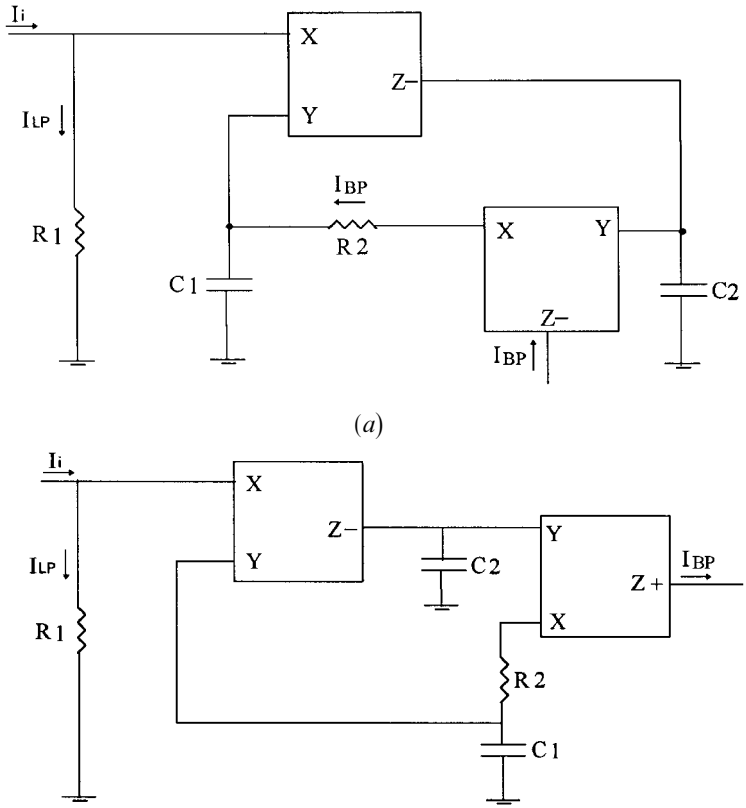

Figure 6. Current-mode grounded-C bandpass filters.

high Q circuit. The current transfer functions are given by

$$\frac{I_{BP}}{I_i} = \frac{sC_1R_1}{s^2C_1C_2R_1R_2 + sC_2R_1 + 1} \tag{8}$$

$$\frac{I_{LP}}{I_i} = \frac{1}{s^2C_1C_2R_1R_2 + sC_2R_1 + 1} \tag{9}$$

For a specified ω_0 and Q, the design equations based on the $R_1C_1 = R_2C_2$ design are given by

$$C_1 = QC_2 \tag{10}$$

$$R_1 = \frac{1}{Q\omega_0C_2} \quad \text{and} \quad R_2 = \frac{1}{\omega_0C_2} \tag{11}$$

It is worth noting that the second CCII can be a CCII+ as well, resulting in the circuit shown in figure 6(b) (Soliman 1997). It should be noted that, although the effect of R_X of the second CCII can be absorbed into R_2, the effect of R_X of the first CCII cannot be easily compensated for. Of course, the stray capacitance C_Z of the first CCII can be absorbed into C_2.

3. The $3R + 2C$ filters

It is well known that the minimum passive component second-order active filters cannot have independent control on the filter Q. In order to have independent control on Q, a third resistor or a third capacitor (Soliman 1996c) must be added to the circuit. In this section a voltage-mode, CFOA-based bandpass-lowpass filter is generated from the passive RLC filter of figure 7(a). Two equivalent current-mode CCII-based bandpass filters (Soliman 1997) are also shown to be related to the same passive RLC filter.

3.1. *Voltage-mode filters*

Figure 7(a) represents the well-known passive RLC lowpass filter whose transfer function is given by

$$\frac{V_{LP}}{V_i} = \frac{1}{s^2LC + sCR_1 + 1} \tag{12}$$

This lowpass filter can be represented by the block diagram shown in figure 7(b), which is equivalent to the two-integrator loop block diagram of figure 7(c), in which

$$T_1 = \frac{L}{R_1} \quad \text{and} \quad T = CR_1 \tag{13}$$

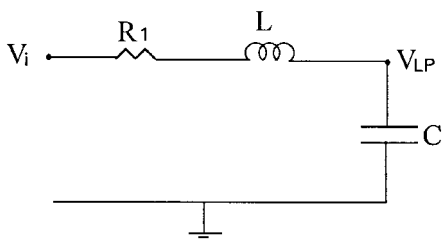

(a)

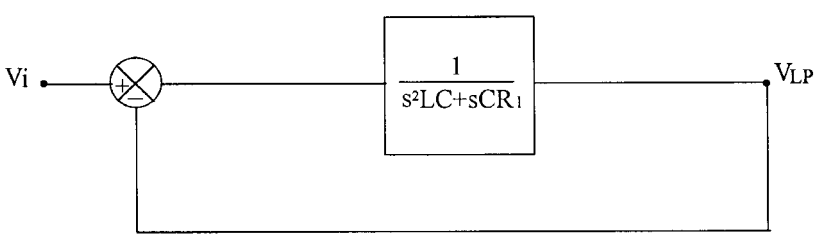

(b)

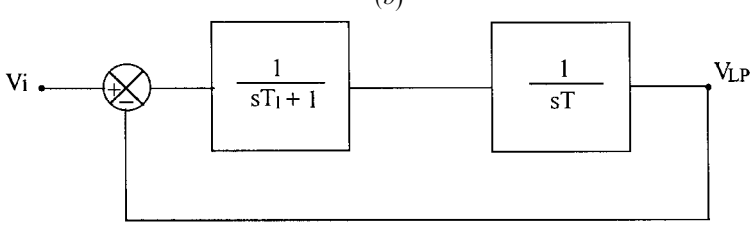

(c)

Figure 7. (a) Passive RLC lowpass filter; (b) block diagram representation; (c) equivalent block diagram based on two integrators.

Two equivalent modified block diagrams are given in figure 8, where

$$a = \frac{R}{R_1} \quad \text{and} \quad T_2 = CR \tag{14}$$

Of course, the resistor R has no physical existence in the circuit of figure 7(a); however, its addition to the modified block diagrams is mainly for the purpose of deriving the equivalent CCII-based filters. The block diagram of figure 8(a) is realized by the CCII-based circuit shown in figure 9, where

$$a = \frac{R}{R_1}, \quad T_1 = C_1 R \quad \text{and} \quad T_2 = C_2 R_2 \tag{15}$$

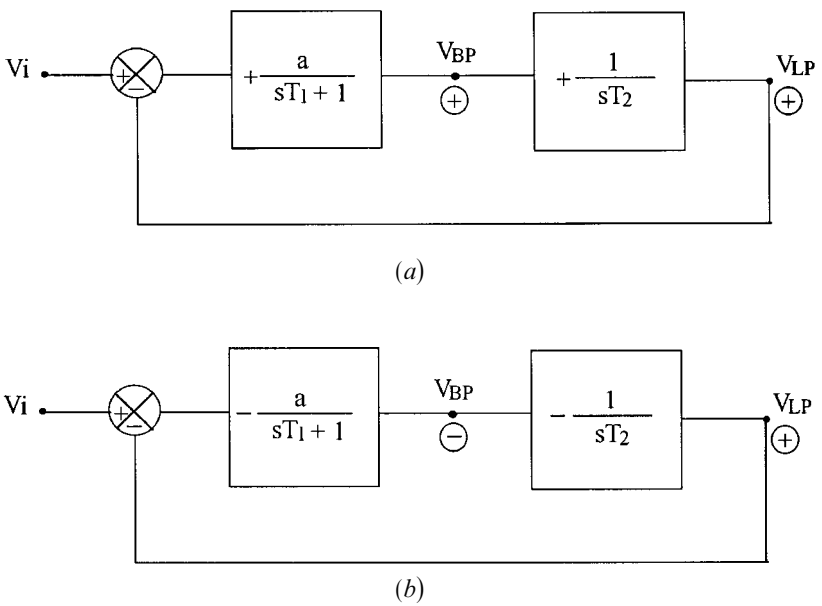

Figure 8. Two equivalent modified block diagrams based on two integrators.

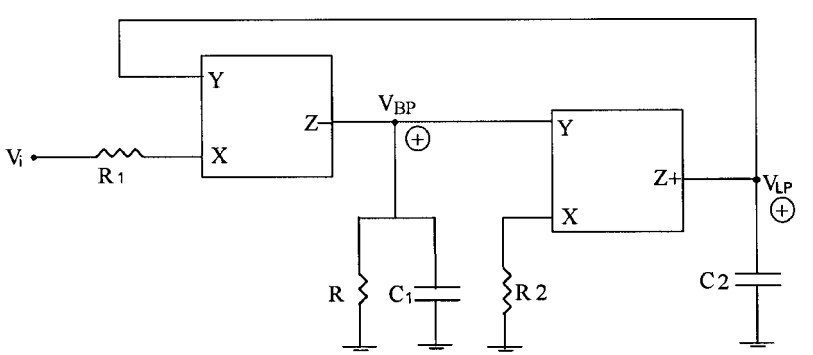

Figure 9. A grounded-C bandpass-lowpass filter using two opposite polarity CCIIs.

The bandpass and the lowpass transfer function are given by

$$\frac{V_{BP}}{V_i} = \frac{\dfrac{s}{C_1 R_1}}{s^2 + \dfrac{s}{C_1 R} + \dfrac{1}{C_1 C_2 R_1 R_2}} \tag{16}$$

$$\frac{V_{LP}}{V_i} = \frac{\dfrac{1}{C_1 C_2 R_1 R_2}}{s^2 + \dfrac{s}{C_1 R} + \dfrac{1}{C_1 C_2 R_1 R_2}} \tag{17}$$

It is seen that the ω_0 and the Q sensitivities to all passive circuit components are ≤ 1 For a specified ω_0 and Q and taking $C_1 = C_2 = C$, the design equations are given by

$$R_1 = R_2 = \frac{1}{\omega_0 C} \quad \text{and} \quad R = \frac{Q}{\omega_0 C} \tag{18}$$

The bandpass center frequency gain is equal to Q, and the lowpass DC gain is unity.

It is worth noting that one of the CCII circuits reported by Liu and Lee (1997) has the same generalized structure as that given in figure 9, with different ports of excitation.

Similarly the block diagram of figure 8(b) in which the bandpass response has inverting polarity can be realized from the circuit of figure 9, by interchanging the two CCII polarities.

It is worth noting that the block diagrams described in figure 8 are different from that used in the generation of the Two-Thomas CCII-based bandpass-lowpass filters (Soliman 1995).

A high input impedance CCII+ based, bandpass-lowpass filter which also realizes the block diagram of figure 8(a) is given in figure 10(a). An equivalent circuit which employs two CFOAs is shown in figure 10(b). The design equations are the same as given by (18). It is worth noting that this circuit is a special case from the recently described circuit of figure 20(b) (Soliman 1996 b).

3.2. *Current-mode bandpass filters*

A current-mode bandpass filter that is related to the passive filter of figure 7(a) is shown in figure 11. The circuit employs a single output CCII- and a balanced output CCII (Elwan and Soliman 1996). This circuit is obtained directly from that of figure 9, by transforming the input voltage source in series with R_1 to a current source I_1 in parallel with R_1 (Soliman 1997). The current transfer function is given by

$$\frac{I_{BP}}{I_i} = \frac{-\dfrac{s}{C_1 R_2}}{s^2 + \dfrac{s}{C_1 R} + \dfrac{1}{C_1 C_2 R_1 R_2}} \tag{19}$$

The design equations are the same as given by (18), and the center frequency gain is equal to $-Q$.

An equivalent current-mode bandpass filter which employs a single output CCII+ and a balanced output CCII can be generated from figure 11 by reversing the CCII polarities.

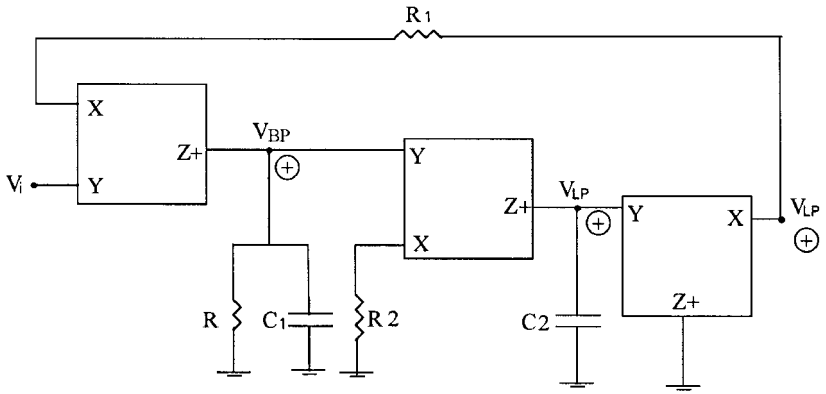

(*a*)

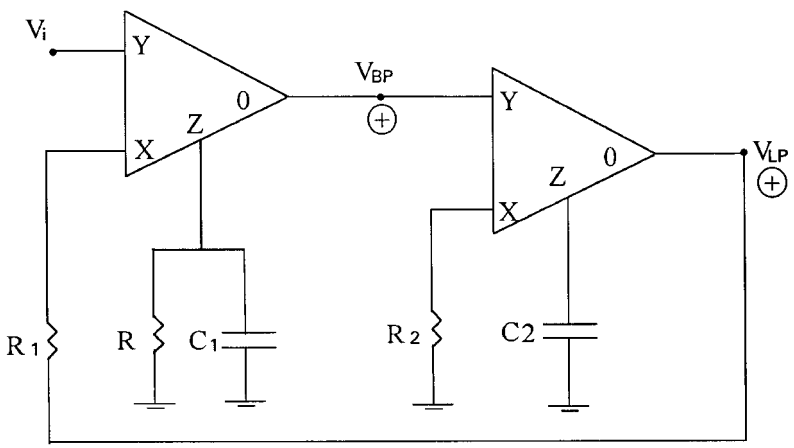

(*b*)

Figure 10. (*a*) A high input impedance bandpass-lowpass filter using three CCII+; (*b*) a non-inverting bandpass-non-inverting lowpass filter using two CFOAs.

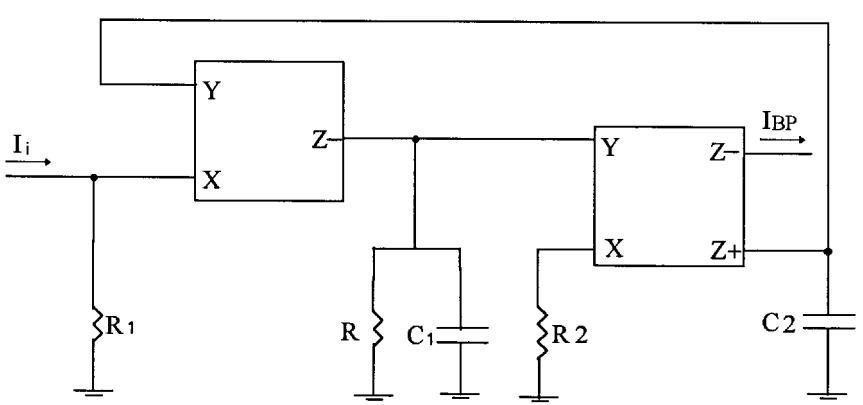

Figure 11. A grounded-*R* grounded-*C* current-mode bandpass filter.

4. PSpice simulation results

PSpice simulations have been carried out using the AD 844 A/AD (Analog Devices 1990) biased with ±9 V. First, the bandpass filter of figure 4 was designed for ω_0 = 1 Mrad/s and Q = 10, by taking C_1 = 0.1 nF, C_2 = 1 nF, R_1 = 1 kΩ and R_2 = 10 kΩ. Figure 12(*a*) represents the magnitude response and figure 12(*b*) represents the phase response. The simulations include the ideal magnitude and the phase responses obtained from a passive *RLC* filter, with a 20 dB added to its magnitude response so that comparison can be achieved. It is seen that there is a small error in the center frequency and in the magnitude and phase characteristics. The errors are mainly due to the resistance R_X and the stray capacitance C_Z of the AD 844, whose values are 65 Ω and 5.5 pF, respectively. Compensation for R_X of each of the CFOAs can be achieved by subtracting its value from R_1 and R_2. Figure 13 represents the magnitude and phase characteristics with R_1 = 0.935 kΩ and R_2 = 9.935 kΩ. The small deviations in the characteristics are due to C_Z of each of the CFOA. Taking C_1 = 94.5 pF and C_2 = 994.5 pF to compensate for the effect of C_Z and with R_1 and R_2 absorbing the effect of R_X, the simulations indicate excellent agreement of both the magnitude and the phase characteristics, as seen from figures 14(*a*) and 14(*b*), respectively.

Next, simulations of the bandpass filter of figure 10(*b*) were carried out using two AD 844A/AD and taking C_1 = C_2 = 1 nF, R_1 = R_2 = 1 kΩ and R = 10 kΩ to realize a bandpass response with ω_0 = 1 Mrad/s and Q = 10. Figure 15 shows the magnitude and phase characteristics. It is seen that the deviation from the ideal response is mainly due to R_X. Figure 16 represents the magnitude and phase characteristics with R_1 = R_2 = 0.935 kΩ, to compensate for the effect of R_X. Additional C_Z compensation by taking C_1 = C_2 = 944.5 pF results in the characteristics shown in figure 17.

Finally, simulations for the current-mode filter of figure 6(*b*) have been carried out using three AD 844A/AD; two of them realize the CCII- . Figure 18 represents the magnitude and phase characteristics obtained with a load R_L = 1 kΩ, and taking C_1 = 1 nF, C_2 = 0.1 nF, R_1 = 1 kΩ and R_2 = 10 kΩ, to realize the same bandpass response with ω_0 = 1 Mrad/s and Q = 10. The responses are compared with the ideal responses obtained from a parallel *RLC* passive filter (with 20 dB added to the magnitude characteristics). Figure 19 represents the compensated characteristics with C_2 = 94.5 pF, R_2 = 9.935 kΩ and with R_1 and C_1 kept at their nominal values of 1 kΩ and 1 nF, respectively.

It should be noted that compensation of the effect of R_X of the first CCII cannot be achieved in a direct form as in the case of the voltage-mode filters.

5. Conclusion

It has been demonstrated that current-mode filters using CCII and voltage-mode filters using CFOA can be generated directly from passive *RLC* filters. New filter circuits using the CCII and the CFOA are generated from three alternative passive *RLC* filters. Compensation of the parasitic parameters of the CCII and the CFOA are considered. PSpice simulation results are included showing the excellent performance of the proposed compensated filters. It should be noted that some of the filters described in this paper have been reported before based on alternative methods of circuit generation.

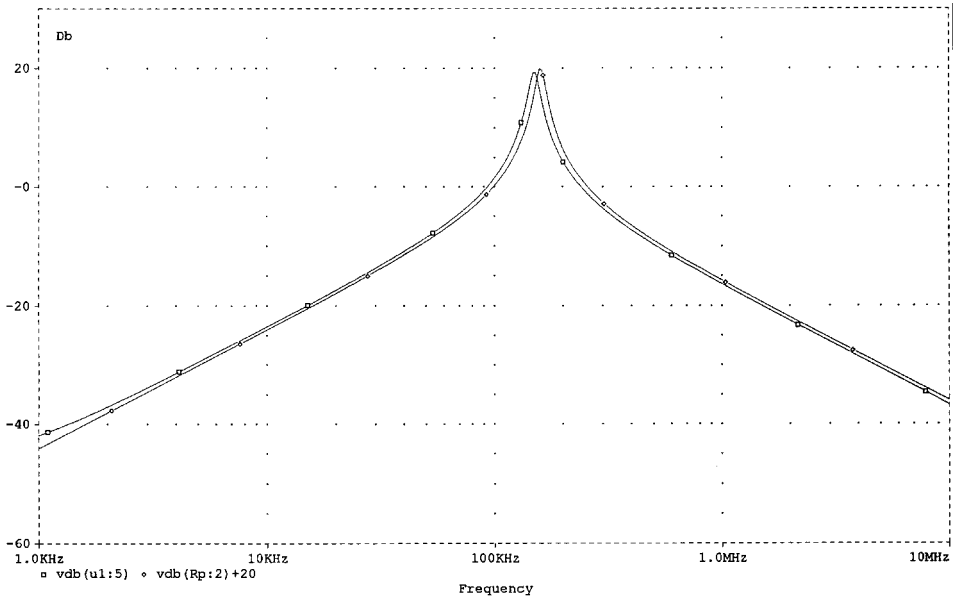

(*a*)

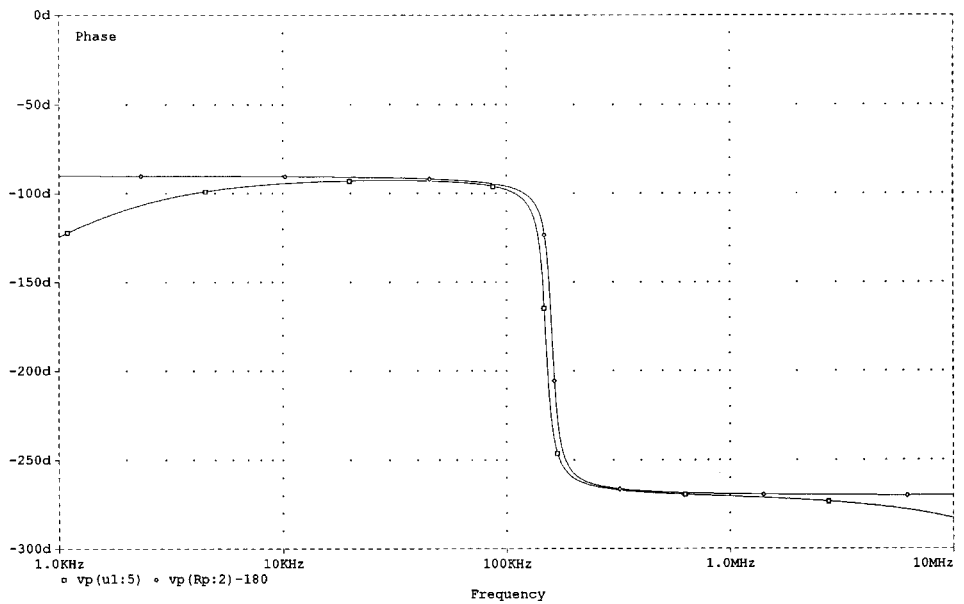

(*b*)

Figure 12. The magnitude and phase characteristics of the bandpass filter of figure 4.

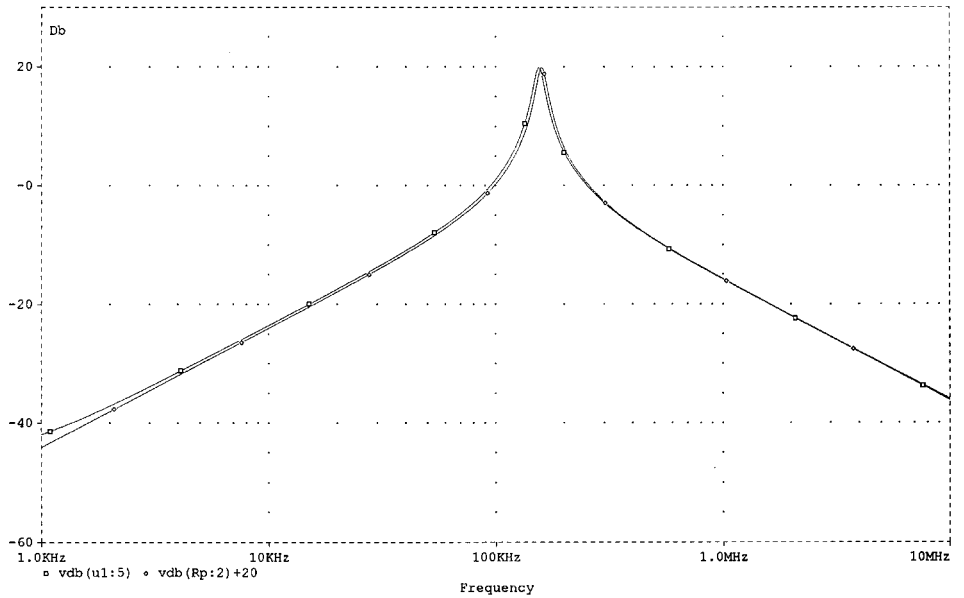

(*a*)

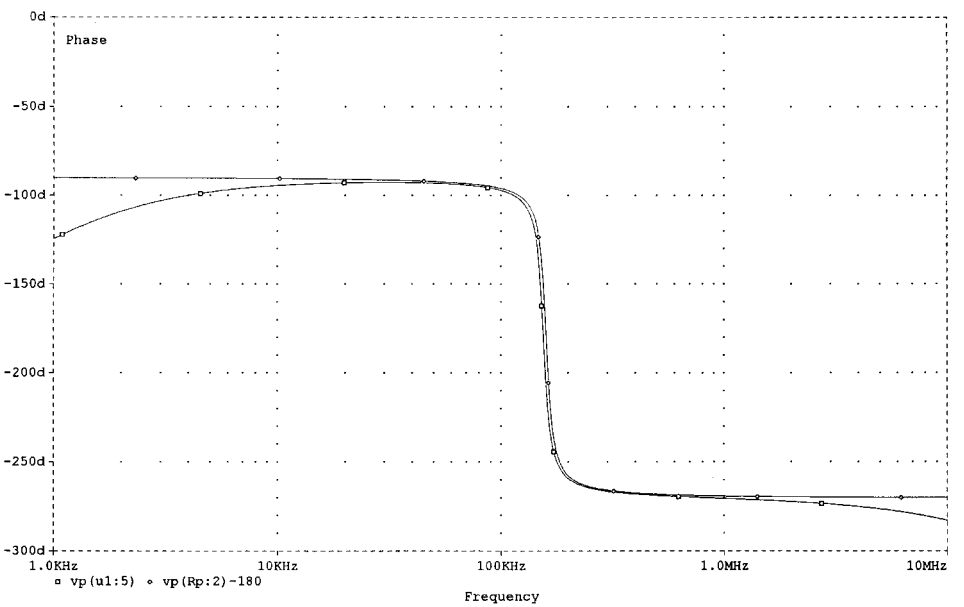

(*b*)

Figure 13. The magnitude and phase characteristics of the R_X compensated bandpass filter of figure 4.

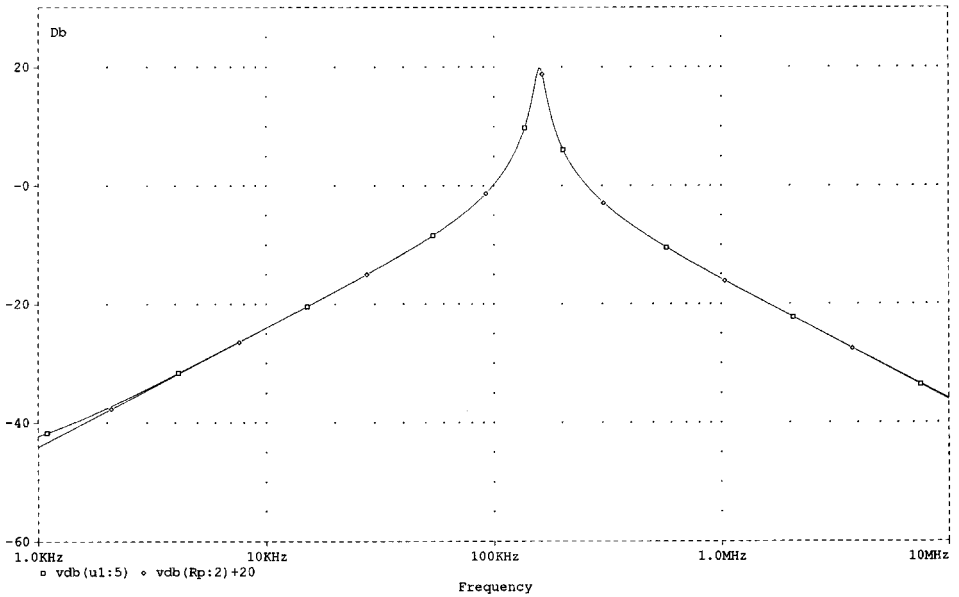

(*a*)

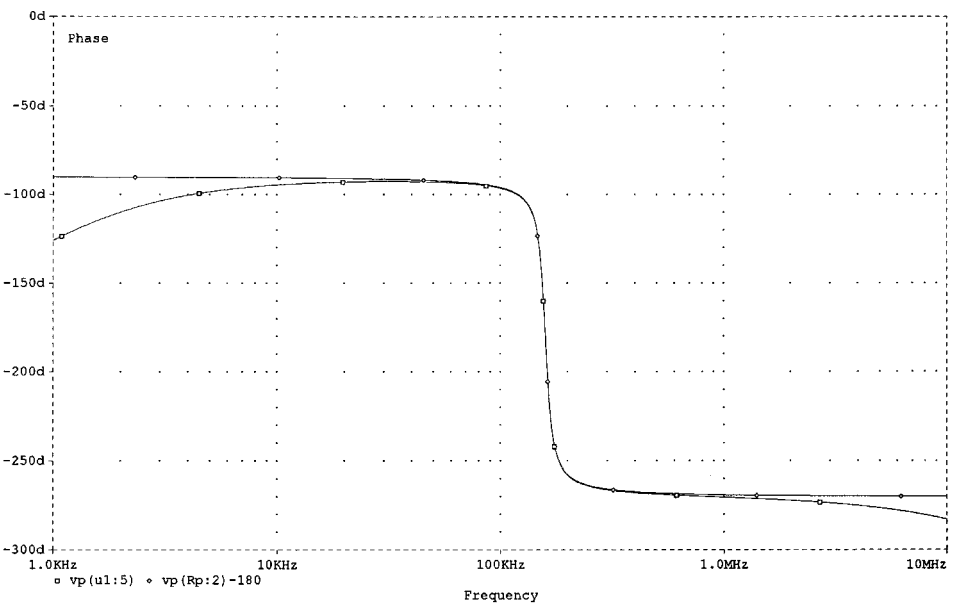

(*b*)

Figure 14. The magnitude and phase characteristics of the R_X and C_Z compensated bandpass filter of figure 4.

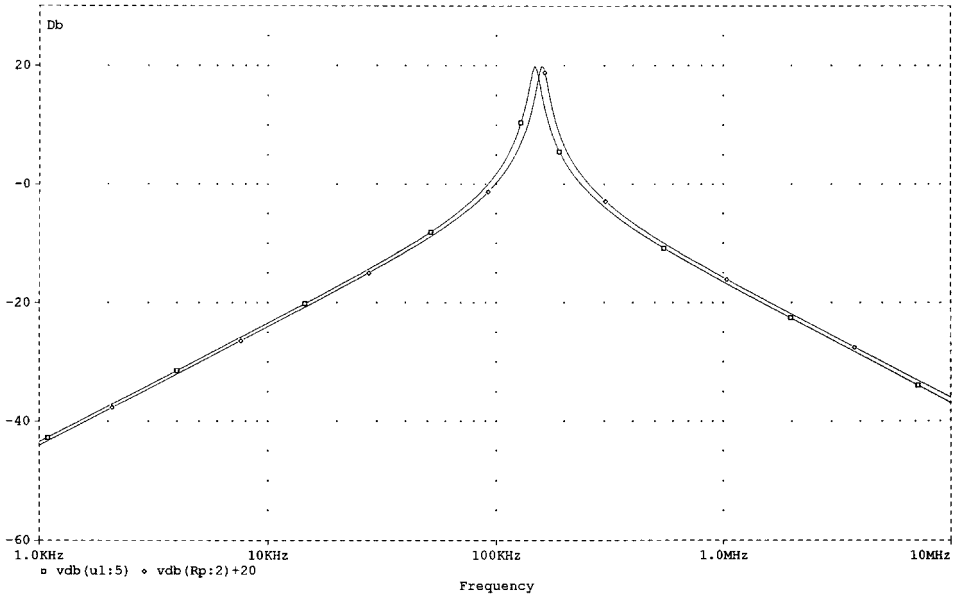

(*a*)

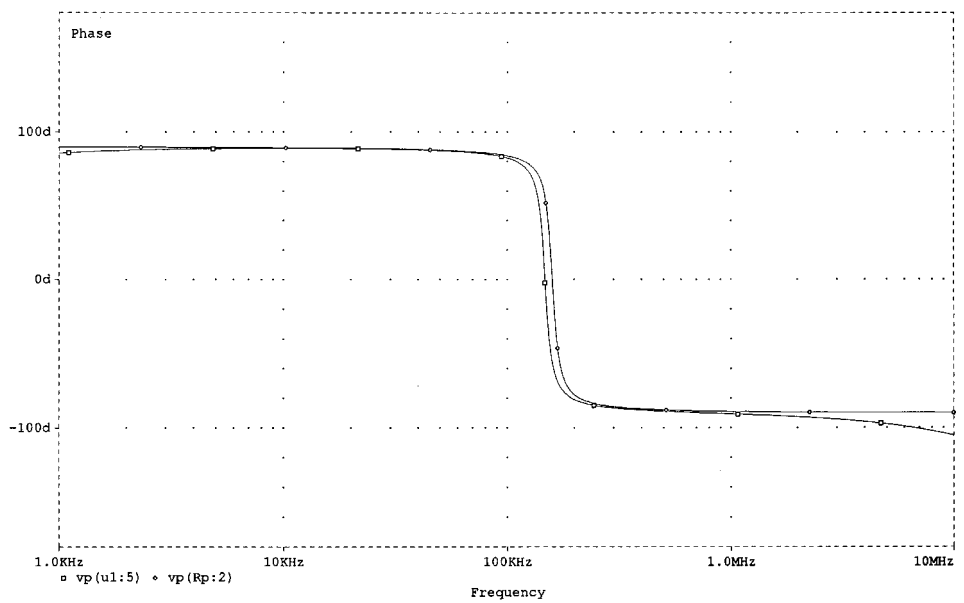

(*b*)

Figure 15. The magnitude and phase characteristics of the bandpass filter of figure 10(*b*).

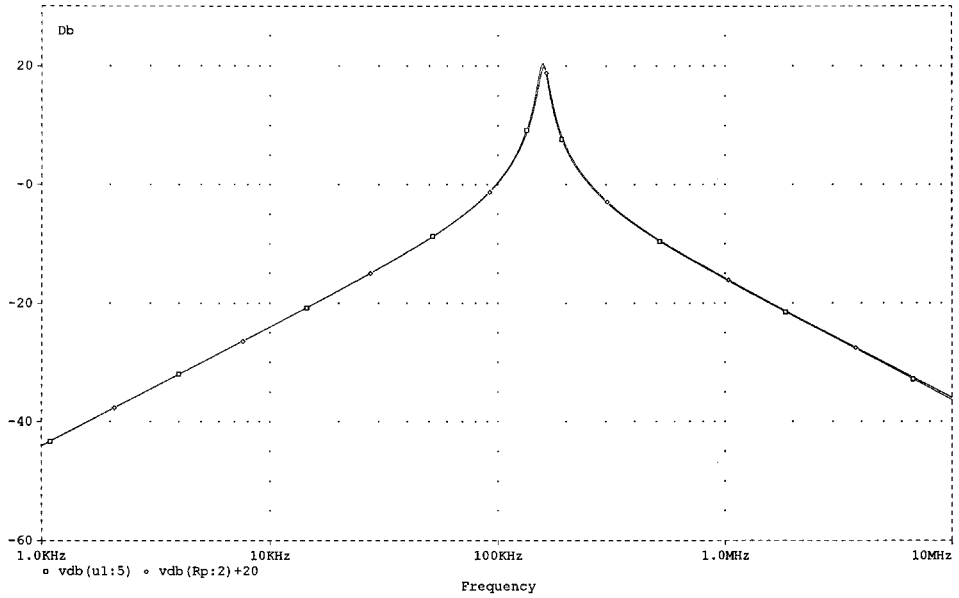

(*a*)

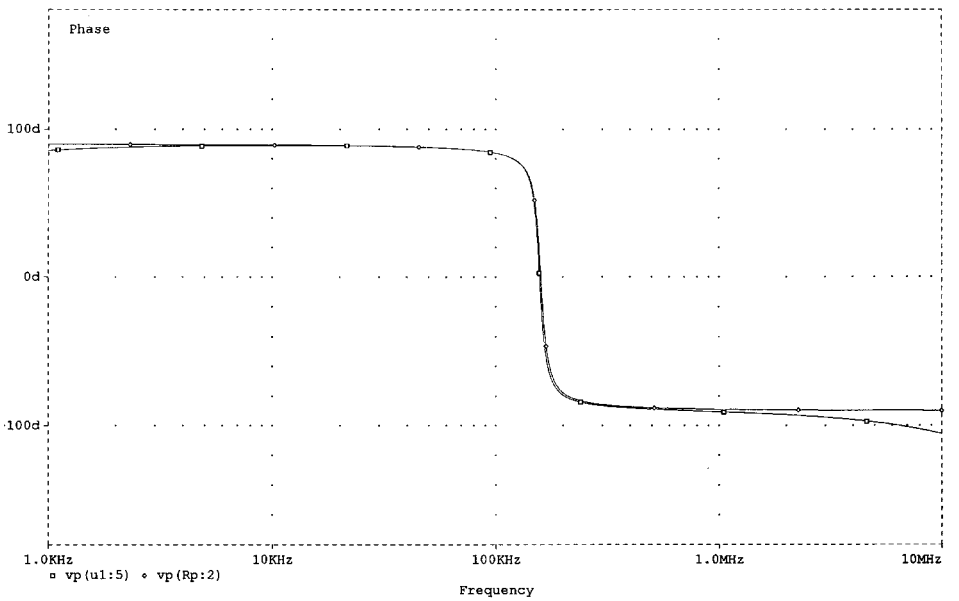

(*b*)

Figure 16. The magnitude and phase characteristics of the R_X compensated bandpass filter of figure 10(*b*).

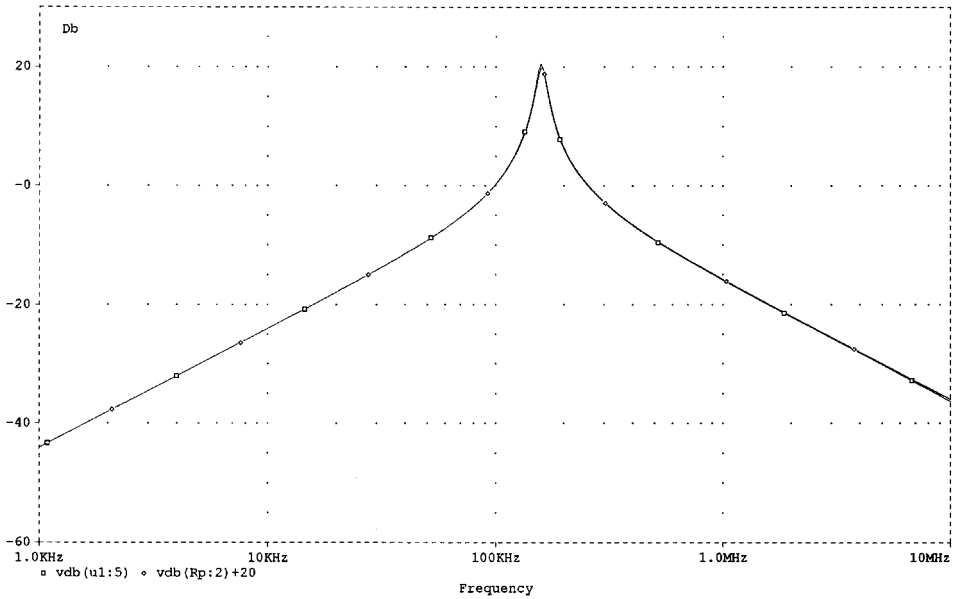

(*a*)

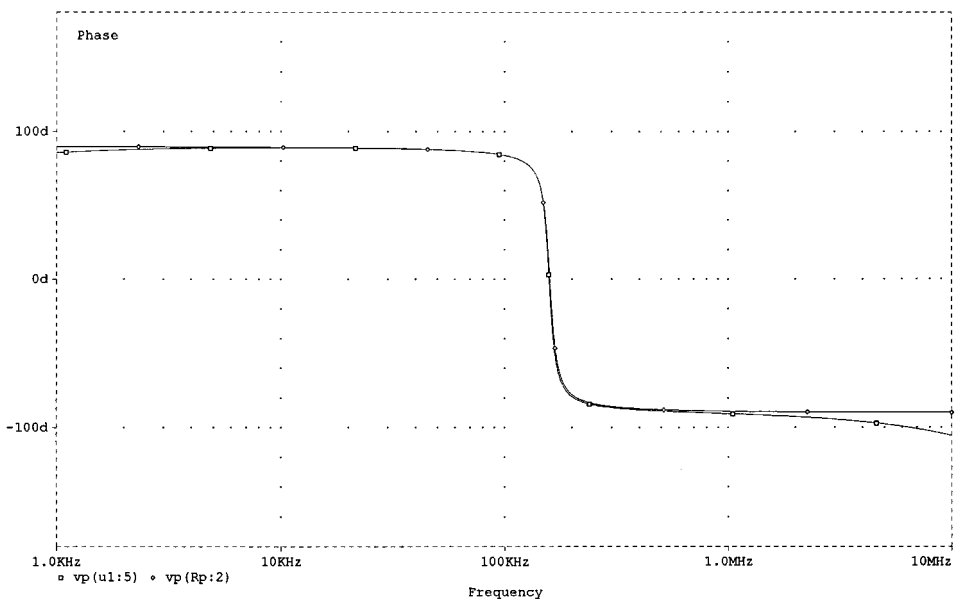

(*b*)

Figure 17. The magnitude and phase characteristics of the R_X and C_Z compensated bandpass filter of figure 10(*b*).

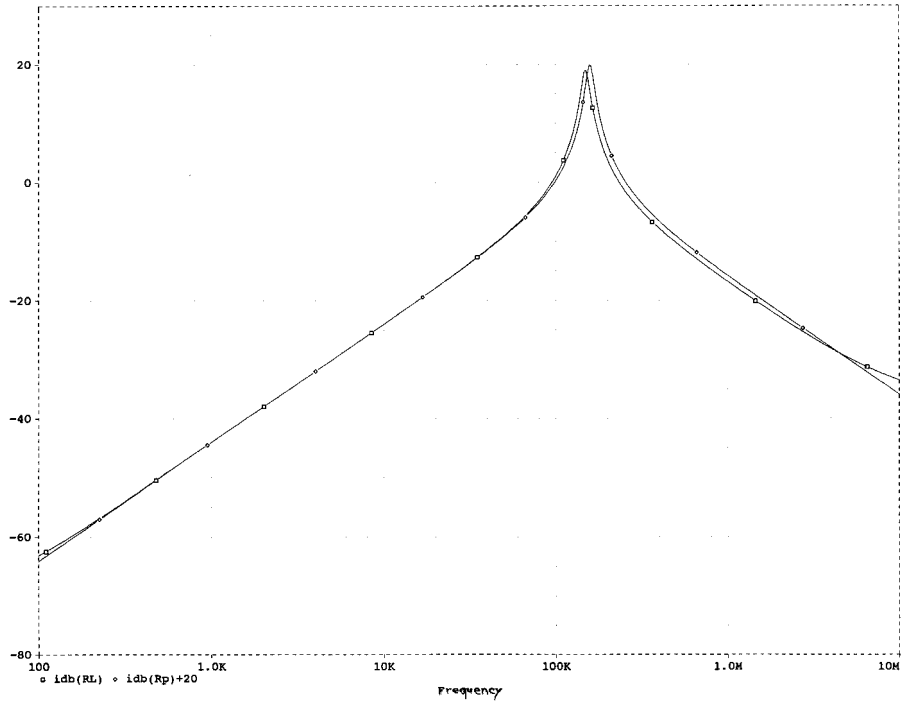

(*a*)

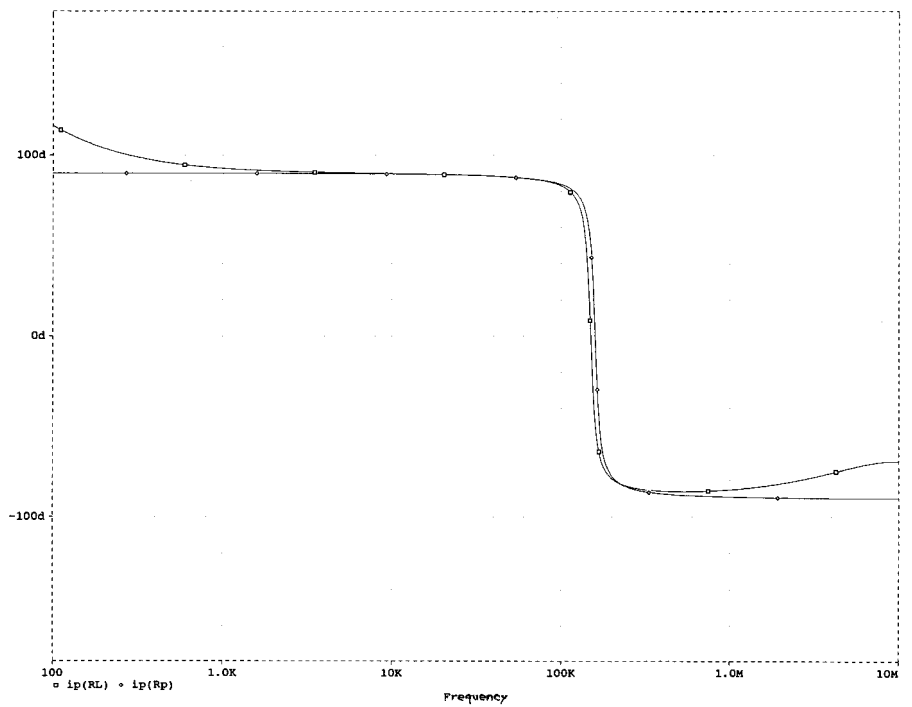

(*b*)

Figure 18. The magnitude and phase characteristics of the current-mode bandpass filter of figure 6(*b*),

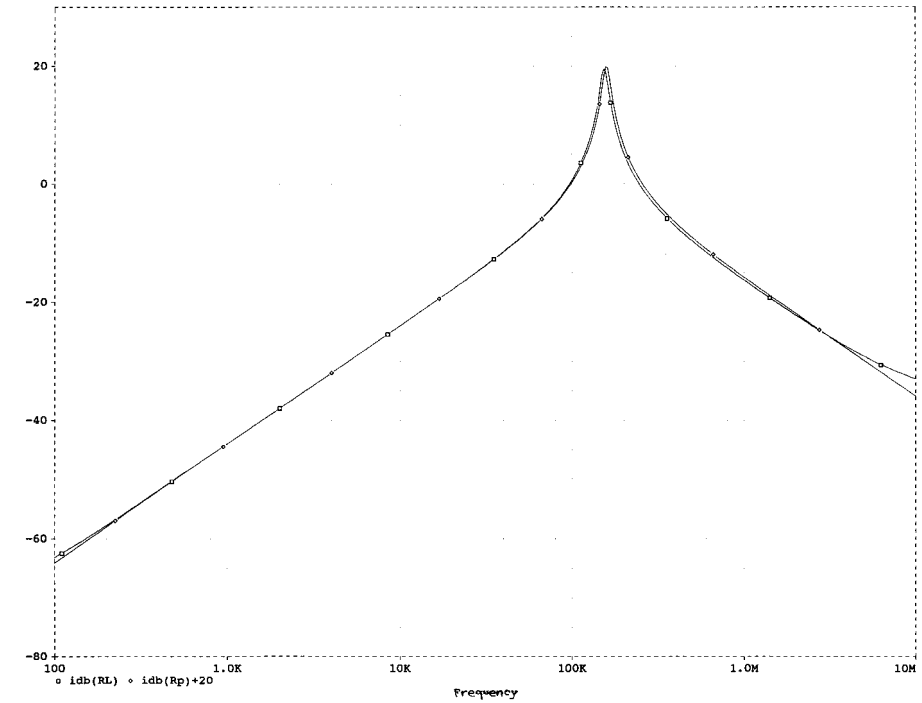

(*a*)

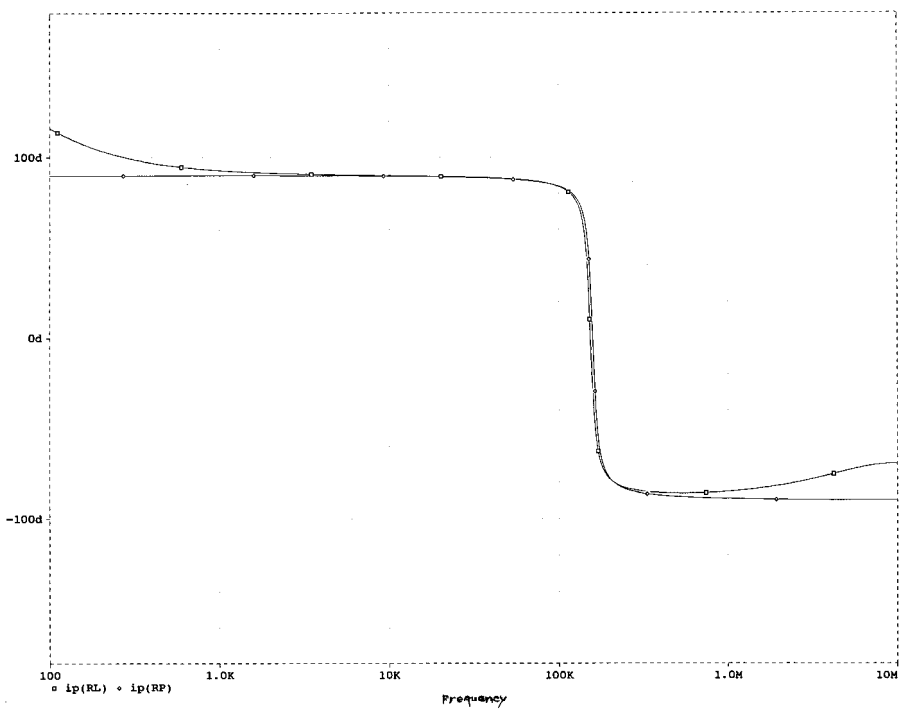

(*b*)

Figure 19. The magnitude and phase characteristics of the compensated current-mode bandpass filter of figure 6(*b*).

References

Abuelmatti, M. T., and Al-Shahrani, S., 1996, New universal filter using two current feedback amplifiers. *International Journal of Electronics*, **80**, 753–756.

Analog Devices, 1990, *Linear Products Data Book* (Norwood, MA: Analog Devices).

Bruton, L. T., 1969, Network transfer functions using the concept of frequency dependent negative resistance. *IEEE Transactions on Circuit Theory*, **16**, 406–408.

Chang, C. M. and Chen, P. C., 1991, Universal active current filter with three inputs and one output using current conveyors. *International Journal of Electronics*, **71**, 817–819.

Chang, C. M., Chien, C. C., and Wang, H. Y., 1994, Universal active current filter with three inputs using current conveyors. *International Journal of Electronics*, **76**, 87–89.

Elwan, H. O., and Soliman, A. M., 1996, A novel CMOS current conveyor realization with an electronically tunable current mode filter suitable for VLSI. *IEEE Transactions on Circuits and Systems*, **43**, 663–670.

Fabre, A., 1992, Gyrator implementation from commercial available transimpedance operational amplifiers. *Electronics Letters*, **28**, 263–264; 1993, Insensitive voltage-mode and current-mode filters from commercially available transimpedance opamps. *Proceedings of the Institution of Electrical Engineers*, Part G, Vol. 140, pp. 319–321.

Higashimura, M., and Fukui, Y., 1996, Universal filter using plus-type CCIIs. *Electronics Letters*, **32**, 810–811.

Liu, S. I., 1995 a, Universal filter using two current feedback amplifiers. *Electronics Letters*, **31**, 629–630; 1995 b, High input impedance filters with low component spread using current-feedback amplifiers. *Electronics Letters*, **31**, 1042–1043.

Liu, S. I., and Lee, J. L., 1997, Voltage mode universal filters using two current conveyors. *International Journal of Electronics*, **82** ,145–149.

Payne, A., and Toumazou, C., 1995, Analogue circuit design using active-*R* current feedback om amps. *Electronic Engineering*, **77**–80.

Roberts, G. W., and Sedra, A. S., 1992, A general class of current amplifier-based biquadratic filter circuits. *IEEE Transactiions on Circuits and Systems*, **39**, 257–263.

Sedra, A., and Smith, K. C., 1970, A second-generation current conveyor and its applications. *IEEE Transactions on Circuit Theory*, **17**, 132–134.

Soliman, A. M., 1978, Ford–Girling equivalent circuit using CCII. *Electronics Letters*, **14**, 721–722; 1994, Kerwin–Huelsman–Newcomb circuit using current conveyors. *Ibid.*, **30**, 2019–2020; 1995, Theorem relating a class of op-amp and current conveyor circuits. *International Journal of Electronics*, **79**, 53–61; 1996 a, New inverting-non-inverting bandpass and lowpass biquad circuit using current conveyors. *Ibid.*, **81**, 577–583; 1996 b, Applications of the current feedback operational amplifiers. *Analog Integrated Circuits and Signal Processing*, **11**, 265–302; 1996 c, New bandpass-lowpass filters using CCII. *Frequenz*, **50**, 181–182; 1997, New current mode filters using current conveyors. *AEU*, **51**, 275–278.

Sun, Y., and Fidler, J. K., 1994, Vesatile active biquad based on second generation current conveyors. *International Journal of Electronics*, **76**, 91–98.

Svoboda, J. A., 1989, Current conveyors, operational amplifiers and nullors. *Proceedings of the Institution of Electrical Engineers*, Pt G, Vol. 136, pp. 317–322.